Spatial Heterogeneity of the Relation Between Resting-State Connectivity and Blood Flow: an Important Consideration for Pharmacological Studies

Najmeh Khalili-Mahani,[1,2,3]* Matthias J. van Osch,[2,4] Mark de Rooij,[1,3] Christian F. Beckmann,[5,6] Mark A. van Buchem,[2,3] Albert Dahan,[7] Johannes M. van Gerven,[8,9] and Serge A.R.B. Rombouts[1,2,3]

[1]*Institute of Psychology, Leiden University, Leiden, The Netherlands*
[2]*Department of Radiology, Leiden University Medical Center (LUMC), Leiden, The Netherlands*
[3]*Leiden Institute for Brain and Cognition (LIBC), Leiden University, Leiden, The Netherlands*
[4]*C. J. Gorter Center for High-field MRI, LUMC, Leiden, The Netherlands*
[5]*Oxford Center for Functional Magnetic Resonance Imaging of the Brain (FMRIB), Oxford University, Oxford, United Kingdom*
[6]*MIRA Institute for Biomedical Technology and Technical Medicine, University or Twente, Enschede, The Netherlands*
[7]*Department of Anesthesiology, LUMC, Leiden, The Netherlands*
[8]*Center for Human Drug Research (CHDR), Leiden, The Netherlands*
[9]*Department of Neurology, LUMC, Leiden, The Netherlands*

◆━━━━━━━━━━━━━━━━━◆

Abstract: Resting state fMRI (RSfMRI) and arterial spin labeling (ASL) provide the field of pharmacological Neuroimaging tool for investigating states of brain activity in terms of functional connectivity or cerebral blood flow (CBF). Functional connectivity reflects the degree of synchrony or correlation of spontaneous fluctuations—mostly in the blood oxygen level dependent (BOLD) signal—across brain networks; but CBF reflects mean delivery of arterial blood to the brain tissue over time. The BOLD and CBF signals are linked to common neurovascular and hemodynamic mechanisms that necessitate increased oxygen transportation to the site of neuronal activation; however, the scale and the sources of variation in static CBF and spatio-temporal BOLD correlations are likely different. We tested this hypothesis by examining the relation between CBF and resting-state-network consistency (RSNC)—representing average intranetwork connectivity, determined from dual regression analysis with eight standard networks of interest (NOIs)—in a crossover placebo-controlled study of morphine and alcohol. Overall, we observed spatially heterogeneous relations between RSNC and CBF, and between the experimental factors (drug-by-time, time, drug and physiological rates) and each of these metrics. The drug-by-time effects on CBF were significant in all networks, but significant RSNC changes were limited to the sensorimotor, the executive/salience and the working memory networks. The post-hoc voxel-wise statistics revealed similar dissociations, perhaps sug-

---

gesting differential sensitivity of RSNC and CBF to neuronal and vascular endpoints of drug actions. The spatial heterogeneity of RSNC/CBF relations encourages further investigation into the role of neuroreceptor distribution and cerebrovascular anatomy in predicting spontaneous fluctuations under drugs. Hum Brain Mapp 00:000–000, 2012.   © 2012 **Wiley Periodicals, Inc.**

INTRODUCTION

The applicability of functional neuroimaging in central nervous system (CNS) drug research has long been advocated [Borsook et al., 2011; Wise and Tracey, 2006], but the challenges of developing a generalizable and robust methodological approach are yet to be overcome [Pendse et al., 2010; Wang et al., 2011]. In recent years, development of task-independent functional neuroimaging has made important strides in neuropharmacology research as it avoids the difficulties of controlling for intersubject variations in task perception and performance under drug and placebo conditions. Importantly, estimating the "resting-state" brain activity facilitates translational research across different species [Margulies et al., 2009; Vincent et al., 2010], making it an appropriate tool in preclinical stages of drug development. Two particular approaches, arterial spin labeling (ASL) and resting-state functional MRI (RSfMRI), have proven applicable in pharmacological neuroimaging [Becerra et al., 2006, 2009; Khalili-Mahani et al., 2011a,b; MacIntosh et al., 2008; Pattinson et al., 2009; Pendse et al., 2010; Rack-Gomer et al., 2009; Wise et al., 2002]. Although the ASL and the RSfMRI signals arise from related neurophysiological sources, these two methods provide different information about the state of brain activity.

Changes in cerebral perfusion are directly linked to overall physiological variations such as cerebral autoregulation and blood pressure control in a systemic process such as the baroreflex [Ogoh et al., 2010]. Different ASL methods (e.g., pulsed or [pseudo]continuous ASL) measure the amount of magnetically tagged arterial blood flowing into the brain tissue, and solve a general kinetic model to estimate the average CBF per unit tissue volume over unit time, with respect to parameters such as blood magnetization, relaxation time, labeling efficiency, and tagging specifics [Buxton et al., 1998]. In Contrast, RSfMRI is used to estimate the temporal dynamics of neuronal oscillations across specific brain networks at "rest," i.e., in the absence of an experimental cognitive task. There are no gold standards for studying resting-state connectivity yet [Cole et al., 2010; Smith et al., 2011]; however, existing evidence suggests that several consistent network topographies emerge form brain signals over time. These topographies are consistently reproducible [Beckmann et al., 2005; Biswal et al., 2010; Damoiseaux et al., 2006]; are detectible even in presence of tasks [Smith et al., 2009]; and correspond to similar networks estimated from electrophysiological fluctuations measured by magnetoencephalography [Brookes et al., 2011]. Therefore, changes in resting-state network connections are interpreted as a proxy for variations in neuronal oscillation in subsets of anatomical regions that serve a particular function. The assumption that resting-state network configurations represent functional connectivity, allows to estimate the consistency of the regional BOLD signal fluctuations with respect to the "representative" oscillations within a functional network of interest. The degree of intranetwork stability can be defined in terms of resting-state network consistency (RSNC), which is a statistical description of how similar the blood oxygen level dependent (BOLD) signal fluctuations are across a particular brain network—after common variations between all other functional networks are factored out.

Although CBF and RSNC metrics are conceptually different, the BOLD signal changes are not independent from CBF. In principle, the BOLD signal arises from a change in the ratio of oxygenated and deoxygenated hemoglobin, which is primarily affected by an influx of oxygenated blood in response to increased metabolic demands of neuronal activation. It is then plausible that the effects detected from these methods converge to some extent. Currently, we lack a knowledge of how the amount of CBF in a given functional network might influence the RSNC, or whether (and how) regional changes in RSNC and CBF correspond under various experimental conditions. This knowledge is particularly critical in interpretation of results from pharmacological studies that, in order to standardize analyses, use canonical resting-state networks as references for estimation of functional connectivity in the rest of the brain.

Limited information about the coupling between BOLD and CBF measures is available from simultaneous acquisition of the BOLD- and CBF change (using dual echo flow-alternating inversion recovery technique) in calibrated-BOLD studies, where the ratio of the BOLD/CBF responses to graded stimuli (visual or sensory stimulations, or physiological stimulations such as controlled hypercapnia or hypoxia) in a specific region of interest is estimated. Under controlled experimental conditions of calibrated-BOLD measurements, a proportional relation between stimulus-induced increase in the BOLD signal and CBF has been reported [Davis et al., 1998; Hoge et al., 1999; Kim et al., 1999]. However, the calibrated BOLD method is based on critical assumptions of cerebral

hemodynamics, i.e., relations between cerebral blood flow, volume and $CMRO_2$ at activation steady-state—and not during spontaneous fluctuations at resting-state. Another critical issue is that the BOLD-related parameters that describe the hemodynamic models used in calibrated BOLD imaging do not consider the influence of the spatial distribution of neurotransmitter receptors [Zilles and Amunts, 2009] on cerebral metabolism—e.g., under drug conditions. In fact, recent applications of calibrated-BOLD under pharmacological interventions indicate that the dynamics of CBF/BOLD coupling across different brain regions may be heterogeneous [Luchtmann et al., 2010; Qiu et al., 2008a,b]. These findings raise further questions about the importance of considering neurochemical and cerebrovascular variations that would lead to spatial heterogeneity of the hemodynamic function and the BOLD/CBF relations.

In resting-state experiments, it is not possible to estimate the BOLD/CBF coupling; however, the spatial distribution of neurotransmitters and the neurovascular anatomy (e.g., the arterial flow territories) may be factors that differentiate functional networks. Quantitative receptor autoradiography indicates that the balance of distribution of different neuroreceptors in different cortical areas plays a role in defining their functional connectivity [Zilles and Amunts, 2009; Zilles et al., 2004]. On the other hand, the hemodynamic function is restricted by the cerebrovascular architecture (i.e., the branching of the vascular tree and the arterial flow territories), which is likely to influence the configuration of the functional networks. Since pharmacological stimuli often act both centrally (at the level of target receptors, where they modulate the neuronal response) and peripherally by inducing global physiological changes in circulation, thus affecting central hemodynamics, they might offer a pragmatic approach to studying the link between local cerebral perfusion and resting-state BOLD signal fluctuations.

Previously, we explored this data to illustrate the effect of different psychoactive substances (morphine and alcohol compared with placebo) on regional perfusion [Khalili-Mahani et al., 2011a] and functional connectivity (which was estimated from dual regression analysis [Beckmann et al.,2009] with respect to representative fluctuations in eight standard resting-state networks [Beckmann et al., 2005; Khalili-Mahani et al., 2011b]). Both methods were sensitive to detecting drug-specific regional effects in brain structures where changes in receptor binding or specific functional control were expected. The most significant effects of morphine on cerebral perfusion were in the anterior cingulate cortex (ACC), the cerebellum, and sensorimotor regions, mostly in the same areas where changes in functional connectivity were detected. In contrast, the effect of alcohol on both functional connectivity and regional CBF was comparatively more limited. These observations motivated the question whether there was a relation between baseline CBF and RSNC within the template networks, and whether these two measures were equally sensitive to predicting drug-by-time interaction
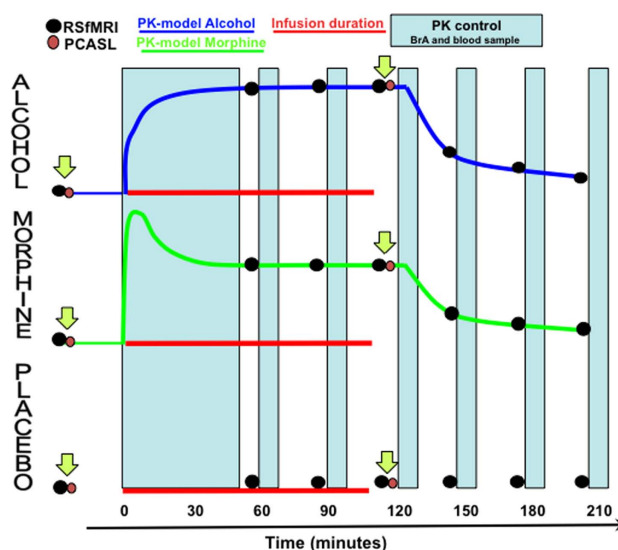

Figure 1.

Schematic experimental design. Arrows indicate the data samples included in dimension-reduced statistical analysis. [Color figure can be viewed in the online issue, which is available at wileyonlinelibrary.com.]

effects on the brain. In this current study, we investigate these questions by first studying the correlations between CBF and RSNC within different NOIs at repeated baseline conditions. Next, we examine whether the same experimental factors explain similar variations in RSNC and CBF across different networks. Finally, we illustrate the dynamics of CBF and RSNC changes in anatomical regions where significant drug-by-time interactions are detected from voxel-based analysis of CBF and RSfMRI data.

MATERIALS AND METHODS

A diagram of the study design is provided in Figure 1.

Subjects

Twelve healthy male participants (age 18–40) volunteered for a randomized double dummy, double blind, placebo-controlled study involving three visits (each one week apart). Exclusion criteria included MRI-contraindications such as implants, pacemakers, or prostheses; any account of medical disorders that could pose a risk to subject's health (e.g., opioid allergy, positive hepatitis B, C, or HIV, cardiac or vascular disorder; asthma or pulmonary disease, major gastrointestinal abnormalities, peptic ulceration, hepatic, neurological, psychiatric, hematological, endocrine, renal, or major genitourinary disease) or jeopardize the aim of the study by introducing confounds (e.g., prevalence of illicit drug use, daily consumption of more than four alcoholic beverages, cigarette smoking, heavy caffeine dependency, and irregular diurnal rhythm).

Pharmacological Procedures

Morphine, alcohol and placebo sessions were randomized. During each visit, subjects experienced identical experimental procedures but in each session different drug compounds (or sham-placebo) were administered intravenously. Glucose 5% solutions were administered as double dummy placebos, where a sham alcohol clamp was performed during the active morphine infusion, and a placebo infusion using the computerized morphine pump was given during the active alcohol clamp (see Fig. 1).

Alcohol Infusion

We aimed for maintaining alcohol levels at 0.6 g/L for 90 min. This was accomplished using the breath alcohol clamping (BrAC) method that provides accurate stable levels of alcohol [O'Connor et al., 1998], as we have previously shown [Zoethout et al., 2008]. Infusion rates required to maintain stable alcohol levels were computed by a nonblind assistant without any other involvement in the study, based on measurements of BrAC at 5-min interval between 0 and 30 min, at 10 minutes intervals between 30–60 min, and 30-min interval between 60 and 300 min after the start of the placebo or drug administration. BrAC was measured outside of the scanner, in the between-scan intervals. The breath alcohol measurement was repeated as a sham procedure during placebo session as well. The nurse assistant kept the subject and the rest of the study team blinded to the recordings.

Morphine Infusion

We aimed to reach stable serum levels of morphine at 80 nmol/L. Morphine infusion was conducted according to pharmacokinetic models established earlier [Sarton et al., 2000]. An initial bolus of 100 µg/kg/h was infused during 1 min; followed by a continuous infusion of 30 µg/kg/h for 2.5 h. Total volume of morphine infusion was ~14.5 mg—a safe dose within the therapeutic range of intravenous morphine for acute pain. To determine the plasma concentration of morphine, venous blood was collected in 5 mL plain tubes (Becton and Dickinson and company, NJ). Blood samples were taken at 0, 15, 30, 50, 60, 90, 120, 150, 180, 210, and 270 min after the start of the placebo or drug administration. All samples were centrifuged for 10 min at 2000 G between 30 and 45 min after collection and stored at −21°C. Plasma concentrations of morphine were determined using liquid chromatography with tandem mass spectrometry [Sarton et al., 2000].

Image Acquisition

Imaging protocols for RSfMRI

A 3T Achieva scanner (Philips Medical System, Best, The Netherlands) was used for image acquisition.

RSfMRI data were obtained using T2*-weighted gradient echo EPI, with TR = 2,180 ms, TE = 30 ms, flip angle = 80°, 64 × 64 × 38 matrix with 3.44 mm isotropic resolution, 220 frames, 8 min; plus a T1-weighted high-resolution scan for anatomical registration. In total, seven sets of RSfMRI were acquired. In each session, only two corresponding ASL data sets were acquired immediately after RSfMRI at times 0 (before infusion began) and 120 min (when the drug concentrations had reached pseudosteady levels). The corresponding measurements that are used in the analyses are pointed out in Figure 1. In statistical tests, when the correlation between RSNC and CBF is examined, we used the two RSfMRI data sets that were acquired immediately before PCASL, in order to minimize any other sources of variations over the time that the drugs had not yet reached steady state. Complete RSfMRI results are published elsewhere [Khalili-Mahani et al., 2011b].

Imaging protocols for PCASL

CBF was measured using PCASL [Dai et al., 2008; van Osch et al., 2009] immediately before and 120 min after drug injection began. Thirty pairs of perfusion weighted and control scans (single shot EPI, 17 slices of 7 mm with an in-plane resolution of 3 × 3 mm^2, SENSE factor 2.5, TE = 13.9 ms at a delay of 1,525 ms, slice time 35 ms, labeling duration 1,650 ms, background inversion pulses at 1,680 ms and 2,760 ms after start of labeling) were obtained (total scan time of 4 min 10 s).

Variables of Interest

Resting-state network consistency

We defined a variable, RSNC, to reflect the degree of stability of fluctuations within a given network of interest (NOI). Our choice of NOIs was based on high reproducibility of these networks from independent component analysis (ICA) of different data sets [Beckmann et al., 2005; Damoiseaux et al., 2006]. Previously, we have shown that this template-based approach allows detecting regional drug-specific effects in functional brain connectivity [Khalili-Mahani et al., 2011b]. To determine RSNC, we performed dual regression analysis to first estimate the temporal profile of the BOLD signal within spatial templates of networks of interest (NOIs, listed in Table I), and next perform a voxel-wise multiple regression analysis to determine how other brain regions are functionally related to these NOIs [Beckmann et al., 2009]. By including all eight networks, the common variations across different networks are partialled out; therefore, the estimated connectivity at each voxel is weighed uniquely to that network. In this way, the averaged connectivity estimates within an NOI provide an index of the fluctuations variance within that network. In other words, if all voxels within a given network fluctuate similarly to the dominant temporal profile of that network, then the RSNC will be

TABLE 1. Template networks of interest

NOI1: Medial visual cortex	Includes, calcarine, inferior precuneus, and primary visual cortex; relays visual input through thalamus to primary visual areas.
NOI2: Lateral visual cortex	Includes lateral occipital cortex (superior and fusiform areas); involved in visual spatial attention.
NOI3: Somatosensory/auditory	Includes superior temporal cortex, insula, operculum, dorsocaudal ACC, somatosensory cortices and bilateral thalamus; involved in bodily awareness and physiological control.
NOI4: Sensorimotor	Includes pre- and postcentral somatosensory somatomotor areas; part of the lateral pain processing system that relay sensory pain signals.
NOI5: default mode	Includes rostral medial PFC and precuneal and PCC areas; linked to readiness for adaptive response to cognitive and emotional tasks.
NOI6: executive control/salience	Includes medial and inferior PFC; implicated in executive control, attention, and salience; includes the medial pain processing system that relays emotional and attentional aspects of pain perception.
NOI7: Left Dorsolateral visual stream/working memory	Includes Broca area 44, frontal pole, dorsolateral PFC and parietal lobule; involved in working memory, visual spatial processing and language.
NOI8: Dorsolateral visual stream/working memory	Includes homologous regions as NOI7, plus right paracingulate gyrus, left PCC and left medial PFC.

NOIs templates are obtained from independent component analysis as described by Beckmann et al., 2005.

high. However, if a given network does not have a consistant temporal profile, i.e., the spontaneous fluctuations across the voxels within that network are highly variable, then the RSNC will be low. An advantage of this approach is that connectivity estimates are robust against common variations in global signal changes (e.g., related to physiological artifacts) [Khalili-Mahani et al., 2012]. Defining a metric that describes the behavior of a template network, independent of global sources of variation, provides a framework for comparing brain activity across sessions, subjects and studies, in a standardized manner.

The details of image processing and analysis are previously described [Khalili-Mahani et al., 2011b]. Briefly, each RSfMRI data set was preprocessed by standard options of FEAT (fMRI Expert Analysis tool, FSL 4.1, fMRIB, Oxford University, UK), including motion correction, brain extraction, linear registration to MNI152 (Montreal Neurological Institute, Montreal, QC, Canada), spatial smoothing with 5

mm blurring kernel and high pass filtering (cut off below 0.01 Hz). Each preprocessed 4D RSfMRI data set was regressed against eight spatial maps (NOIs), to produce eight vectors representing the estimated BOLD fluctuations in each NOI over the scanning period. In the second regression, each 4D RSfMRI data set was regressed against the eight timecourse vectors, together with motion parameters, to generate 8 RSNC maps. We performed no mean normalization in either stage of the regression. Since retrospective physiological correction did not change the average RSNC within each NOI [Khalili-Mahani et al., 2012], we used the uncorrected data to estimate functional connectivity. The value of each voxel in the map corresponds to the z-score of the "fit" of a given template timecourse, to fluctuations at each voxel of the brain image. We refer to RSNC in terms of the absolute value of z-score in each voxel, representing how well that voxel is "connected" to the NOI.

Cerebral blood flow

For each set, voxelwise CBF was computed using

$$CBF(x,y,z) = 6000 \frac{\sum_{t=1}^{N}(S_{control}(x,y,z,t) - S_{label}(x,y,z,t))}{N} \frac{1}{labelingfficiency \times M_0 T_1 blood \times \lambda} e^{\left(\frac{delay+slicetime(z-0.5)}{T_1 blood}+\frac{TE}{T_2}\right)}$$

where N 30, λ 0.76, labeling efficiency 0.85, TE 13.9 ms, T_2 50 ms and T_1blood 1,680 ms. These computations were performed using MATLAB R2009a (Mathworks). Having computed CBF in native space for subjects, we spatially standardized them to the MNI152 template (using FLIRT, FMRIB's linear registration tool, FSL4.1, Oxford University, UK) in order to be able to perform group-level statistical inference testing. The same blurring kernel as used for RSfMRI was used for spatial smoothing. For methodological details see [Khalili-Mahani et al., 2011a].

The CBF values are computed in units of ml/100 ml-tissue/min.

Reducing data dimension in NOIs

The spatial data across each NOI was reduced by averaging the voxelwise RSNC (i.e., z-scores obtained from dual regression analysis described above) and the CBF values within a binarized mask of each template NOI. The binarized masks are confined to regions within consistency

threshold of $|z| > 3.1$ (voxel-wise $P > 0.001$). Although this data reduction approach limits the ability to detect drug effects in anatomical structures, it helps standardize statistical model testing for examining the heterogeneity of RSNC/CBF relations across different experimental conditions and different independent studies. To ensure this limitation does not obscure important variations in inter- and extra-NOI relations between the BOLD signal fluctuations and the CBF, we have also performed voxelwise statistics and a post-hoc conjunction analysis on the MRI data.

Physiological confounds

Physiological data were measured during RSfMRI scanning using standard scanner equipment. We averaged the heart rate over the period of each scan. The respiratory signal over the scanning period was low-pass filtered (cutoff frequency 5 Hz) and the highest harmonic of the Fourier transformation of the respiration signal was used as a representative average respiration rate during the scan.

It has been shown that altered respiration due to opiate treatment leads to a hypercapnia-related increase in CBF [MacIntosh et al., 2008; Pattinson et al., 2007]. Also, heart rate increase due to alcohol might be associated with vaso-reactive changes that alter the arterial blood flow velocity [Blaha et al., 2003]. We have previously shown that respiration rate explains about 17% of variation in global CBF [Khalili-Mahani et al., 2011a], and that the extent of morphine effects on some NOIs is changed if respiration rate is included in the GLM as a confound regressor [Khalili-Mahani et al., 2011b]. Therefore, average heart rate and dominant respiration rates (obtained from spectral analysis of the respiration signal) are included in the following statistical analyses in order to account for correlated global signal changes in all networks.

Statistical Tests

Repeated-measures analysis of correlation between CBF and RSNC

Statistical analysis was done using generalized estimating equations (GEE)—a special form of the general linear model (GLM) that accounts for correlations between repeated measurement from each subject, in order to avoid incorrect estimation of the standard error of regression parameters [Liang and Zeger, 1986; Zeger et al., 1988]. The following GEE models were examined (B's refer to parameter estimates, and i refers to the index of the NOI):

Relation between RSNC and CBF at baseline

For i in NOI1 to NOI8;

$$Y\text{Baseline}_{\text{RSNC}}(i) = B_0(i) + B_1(i)\ \text{BaselineCBF}(i) + B_2(i)\ \text{respiration} + B_3(i)\ \text{heart (Model 1)}$$

Relation between RSNC and CBF under pharmacological conditions

For i in NOI1 to NOI8;

$$Y_{\text{RSNC}}(i) = B_0(i) + B_1(i)\ \text{time} + B_2(i)\ \text{condition} + B_3(i)\ (\text{time} \times \text{condition}) + B_4(i)\ \text{respiration} + B_5(i)\ \text{heart} + B_6(i)\ \text{CBF}(i)\ \text{(Model 2)}$$

Effect of Experimental factors on RSNC and CBF

For i in NOI1 to NOI8;

$$Y_{\text{RSNC}}(i) = B_0(i) + B_1(i)\ \text{time} + B_2(i)\ \text{condition} + B_3(i)\ (\text{time} \times \text{condition}) + B_4(i)\ \text{respiration} + B_5(i)\ \text{heart (Model 3A)}$$
$$Y_{\text{CBF}}(i) = B_0(i) + B_1(i)\ \text{time} + B_2(i)\ \text{condition} + B_3(i)\ (\text{time} \times \text{condition}) + B_4(i)\ \text{respiration} + B_5(i)\ \text{heart (Model 3B)}$$

In all models above, correlation was assumed within subjects. Variables time (pre, post) and condition (placebo, morphine, alcohol), and NOI (1, 2, 3, 4, 5, 6, 7, and 8) were categorical. Variables respiration, heart (the dominant respiration frequency, and average heart rates measured over scanning period), CBF (average CBF in each NOI) and RSNC (average Z-scores of dual regression in each NOI) were normally distributed. Because the volume of different NOIs and the amount of gray matter in each is different, we averaged the gray matter (GM) partial volume effect (obtained using FSLs FAST tool, for each of the three anatomical images per visit) within each NOI mask and included the values as a weighting factor in all GEE models above. Baseline measure refers to the preinfusion measurements in each visit day. The standard errors of the estimates were computed using robust Sandwich estimates assuming an exchangeable working correlation form. We used a corrected alpha level of $0.05/8 = 0.006$, to account for multiple comparisons with eight networks. Because of the exploratory nature of the study, we like to control the number of Type II errors; therefore we refrained from using a more stringent level by correcting for the number of all tests. Also, because our main interest is in the relation between CBF and RSNC, such results with $P > 0.05$ will be reported as a trend. All statistical tests were done using IBM SPSS 18.0 for MAC (IBM Co., Somers, NY).

Voxel-Wise Conjunction Analysis

Results of dimension-reduced data would lack anatomical specificity. Considering the heterogeneous relations observed above, we examined the drug effects observed in voxel-wise statistical parametric maps reported before [Khalili-Mahani et al., 2011a,b]. We performed conjunction analysis [Nichols et al., 2005] to illustrate the focal dynamics of change in CBF and connectivity in the brain areas affected by drugs. Conjunction maps were obtained from statistical

TABLE II. Drug concentrations at the time of post-infusion MRI scan

Subject	Morphine nmol/L	Ethanol mg/L
1	67	500
2	63	470
3	81	540
4	70	540
5	63	560
6	63	640
7	70	640
8	67	580
9	74	590
10	63	650
11	60	660
12	63	690

parametric maps (mixed effect analysis of drug and time interactions, obtained from a 5,000-permutation testing). Statistical maps were cluster-thresholded at $P < 0.05$. To account for multiple comparisons across 8 NOI, a cluster forming threshold of $P < 0.001$ was used. The values of the significant loci were plotted to illustrate the heterogeneity of the dynamics of CBF and RSNC across different brain regions.

Note that a permutation test of RSfMRI data at two timepoints (acquired at the same time as the corresponding CBF data) did not provide effects that satisfied statistical criteria. Since the objective of this post-hoc analysis is to examine the dynamics of these two metrics in anatomical loci where significant drug effects were observed, we performed the conjunction analysis on significant statistical results from seven RSfMRI datapoints.

RESULTS

Plasma Drug Concentrations

Table II lists the plasma concentration for each drug in each subject at the time point when CBF and RSN scans were made (rounded). At the time of post-treatment scan, average morphine levels were at 68.04 ± 8.8 nmol/L and average alcohol levels were at 0.63 ± 0.038 (g/L).

Relation Between CBF and RSNC in Baseline Conditions

We examined how much of the variation in repeated baseline measurements of RSNC in each NOI was explained by the corresponding CBF variations (Model 1). Results are presented in Table III. A trend for association between baseline RSNC and baseline CBF was observed in the somatosensory (NOI3), sensorimotor (NOI4) and the default mode network (NOI5) (P's < 0.04). Significant respiratory effects on sensorimotor network (NOI4) and significant heart rate effects on the lateral visual network (NOI2) were observed (P's < 0.006).

Relation Between CBF and RSNC in NOIs Under Pharmacological Conditions

In Model 2, we tested whether variation in CBF under experimental conditions predicted significant RSNC variations in each NOI. Figure 2 illustrates a heterogeneous pattern of relations between CBF and RSNC across different networks and conditions as estimated by GEE.

A significant effect of CBF on RSNC was observed in NOIs 6 and 7, where higher CBF values were associated with smaller RSNC magnitude (see Table IV).

Effects of condition x time interaction estimated from Model 2 show a trend only in NOI4 ($P < 0.03$). Main effect of time is significant in NOIs 2, 3, 5, and 8 and a trend is present in NOIs 6 and 7. Main effect of condition showed a trend only in NOIs 4 and 6.

Differences and Similarities of Drug Effects on CBF and on RSNC

Figure 3 illustrates that the effect of drugs on average RSNC and average CBF is not the same across the networks. In Model 3 we examined whether a given explanatory model would predict similar effects on CBF and on RNCS across different NOIs. A plot of the quasi likelihood under independence (QIC) model criterion [Pan, 2001] illustrates that the predictive power of such a model across different NOIs is not similar (i.e., not a flat line) and,
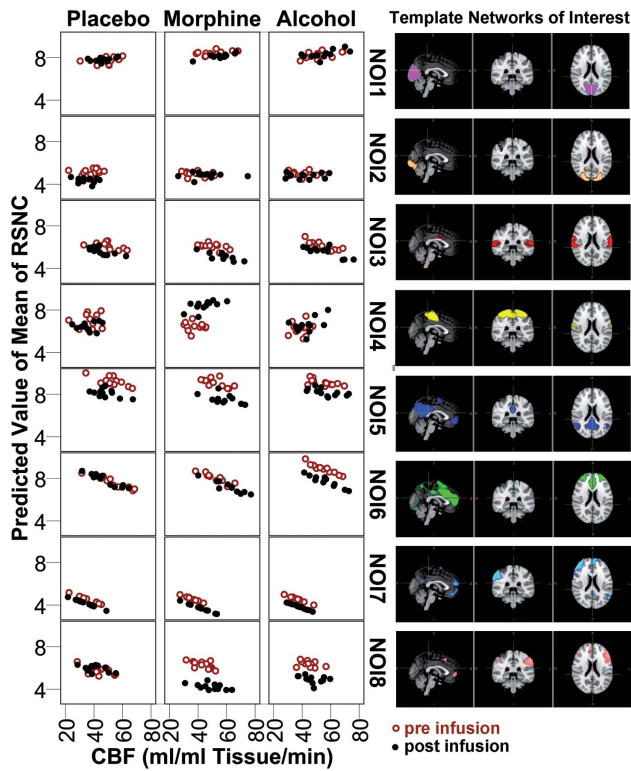
TABLE III. Estimated effect of physiological factors and CBF on RSNC at baseline

Variable		NOI1	NOI2	NOI3	NOI4	NOI5	NOI6	NOI7	NOI8
Intercept	Wald χ_2 (df = 1)	2.716	98.535	26.150	1.365	17.427	12.557	13.749	3.247
	P	0.099	0.000	0.000	0.243	0.000	0.000	0.000	0.072
CBF	Wald χ_2 (df = 1)	3.139	0.014	4.218	4.302	5.091	0.453	1.196	1.184
	P	0.076	0.906	0.040	0.038	0.024	0.501	0.274	0.276
Respiration	Wald χ_2 (df = 1)	1.219	2.706	1.154	7.599	0.008	0.318	1.796	3.263
	P	0.270	0.100	0.283	0.006	0.930	0.573	0.180	0.071
Heart rate	Wald χ_2 (df = 1)	3.192	13.584	1.716	2.438	2.808	0.641	0.067	0.093
	P	0.074	0.000	0.190	0.118	0.094	0.423	0.795	0.760

Model 1: Intercept + respiration + heart-rate + CBF.
$P < 0.05$ (trend); $P < 0.006$ (significant, corrected for multiple comparisons).

Figure 2.

Estimates of variations in RSNC (from a GEE model including drug × time interactions, plus heart rate and respiration) plotted versus CBF. [Color figure can be viewed in the online issue, which is available at wileyonlinelibrary.com.]

maybe more importantly, that the influence of explanatory variables is not homogeneous for RSNC and CBF as can be assessed from the fact that the two lines are not parallel (Supporting Information Fig. 1). (Note that QIC is a

method for comparing the predictive power of different models. Usually it is used to determine the most parsimonious model that best describes an independent variable. Here, we use QIC only for illustrative purposes, to show the between-network heterogeneities.)

Statistical results are provided in Supporting Information Table I and illustrate that variations in CBF and RSNC are not always explained by the same factor.

In summary, condition × time interactions showed effect trends on variations of RSNC in sensorimotor (NOI4), salience/executive (NOI6), and dorsolateral visual and working memory (NOI8) networks. Main effect of time on RSNC was significant in all networks except in visual and sensorimotor networks (NOI1 and NOI4), albeit the time effect on NOI6 was a trend.

In contrast, condition × time interaction explained significant variations in the CBF in all NOIs (P's < 0.001). The effect of condition on CBF was significant in NOI4 but a trend was present in all other NOIs (P's < 0.05) other than NOI8.

Post-Hoc Conjunction Analysis of Local Changes in CBF and RSNC

Supporting Information Tables II and III list brain areas where conjunction analysis on statistical parametric maps of morphine and alcohol effects revealed overlapping effects on RSNC and on CBF for each drug. Plotted peaks at some regions of interest illustrate the heterogeneity of CBF/RSNC relations (Fig. 4). The largest overlap (in terms of the magnitude of the affected clusters) was observed in connectivity of NOI4 (sensorimotor network and part of the lateral pain system) and NOI6 (attention and salience network and part of the medial pain system) in response to morphine (Supporting Information Table II) and in connectivity of NOI1 (medial visual network) and NOI3

TABLE IV. Effects of experimental factors on RSNC of each NOI

Variable		NOI1	NOI2	NOI3	NOI4	NOI5	NOI6	NOI7	NOI8
(Intercept)	Wald $\chi^2_{\,df=1}$	13.88	30.53	37.21	6.39	13.76	31.17	14.09	8.00
	P	0	0	0	0.011	0	0	0	0.005
Time	Wald $\chi^2_{\,df=1}$	0.13	14.68	9.05	0.17	16.89	4.33	6.28	11.19
	P	0.724	0	0.003	0.684	0	0.037	0.012	0.001
Condition	Wald $\chi^2_{\,df=2}$	4.03	0.47	3.82	7.65	0.78	7.54	0.05	1.04
	P	0.133	0.792	0.148	0.022	0.677	0.023	0.974	0.596
Time x Condition	Wald $\chi^2_{\,df=P}$	0.16	2.86	2.67	7.70	0.05	2.53	0.47	5.21
	P	0.922	0.24	0.263	0.021	0.975	0.282	0.79	0.074
Respiration	Wald $\chi^2_{\,df=1}$	1.45	0.80	3.85	6.91	1.63	0.24	0.00	3.90
	P	0.228	0.372	0.05	0.009	0.201	0.624	0.948	0.048
Heart rate	Wald $\chi^2_{\,df=1}$	0.33	8.24	0.84	4.15	3.00	0.54	0.01	0.48
	P	0.564	0.004	0.36	0.042	0.083	0.464	0.913	0.487
CBF	Wald $\chi^2_{\,df=1}$	1.32	0.03	3.17	2.26	2.19	8.61	8.27	2.26
	P	0.251	0.861	0.075	0.132	0.139	0.003	0.004	0.132

Model 2: Intercept+ time + Condition + time x Condition + respiration + heart rate + CBF.
$P < 0.05$ (trend); $P < 0.006$ (significant, corrected for multiple comparisons).
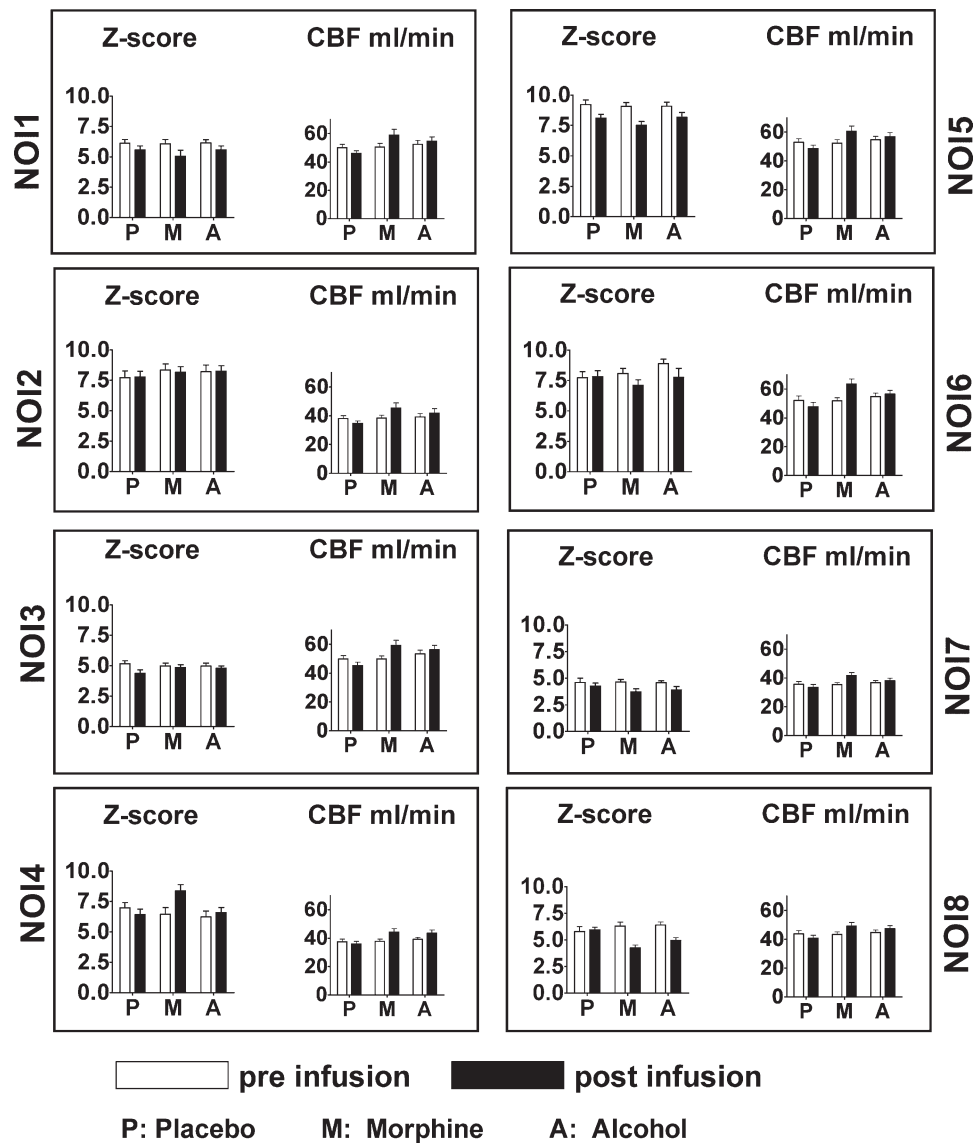
Figure 3.
Average RSNC and average CBF values within different NOIs at each timepoint for each drug condition.

(somatosensory network) in response to alcohol (Supporting Information Table III).

As Figure 4 illustrates, the patterns of drug-by-time interactions with CBF and RSNC are not uniform. In case of morphine, three different interactions emerged: Increase in both RSNC and CBF, compared to placebo and baseline in the central sulcus (Fig. 4A); increase in negative RSNC and increase CBF in the hippocampus (Fig. 4B); and decreased RSNC in the anterior cingulate cortex (ACC) with increased CBF (Fig. 4C).

The overlapping alcohol effects were in general more limited (Supporting Information Table III), because smaller changes in voxel-wise RSNC were detected. The effects of alcohol were exclusive to small regions where a drug-by-

time interaction effect on NOI1 (visual), NOI3 (somatosensory and auditory) and NOI4 was present. As Figures 4D,E illustrate, the observed effect was mainly driven by a difference between alcohol and placebo condition. The direction of CBF and RSNC effects in medial visual and paracingulate cortex, where strongest effects were observed, were similar.

DISCUSSION

Previously, we have shown that resting-state functional connectivity (obtained from NOI-based dual regression analysis of RSfMRI) and cerebral perfusion (obtained from
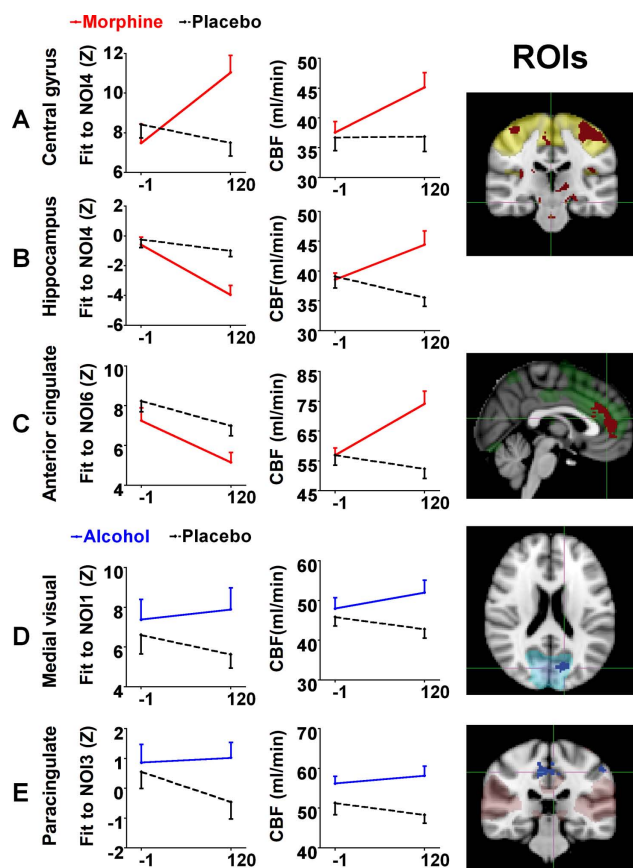
Figure 4.

Post-hoc analysis of overlapping changes in CBF and RSNC with respect to placebo at $t = -1$ min (before infusion) to $t = 120$ min (after drugs reach pseudo steady levels) in selected ROIs ($P > 0.05$, corrected). (**A**) Similar direction of effect in central gyrus; (**B**) emerging negative connectivity and increased CBF in the hippocampus (**C**) Opposite direction of change in CBF and connectivity in perigenual ACC; (**D** and **E**) similar alcohol effects on CBF and connectivity in medial visual and paracingulate cortices. [Color figure can be viewed in the online issue, which is available at wileyonlinelibrary.com.]

PCASL measurements) are promising markers for studying regional and drug-specific changes in brain function. Here, we have taken a prototypical approach to studying the CBF and RSNC within eight prominent resting-state networks to test the hypothesis that functional connectivity and cerebral blood flow were sensitive to different aspects of functional cerebral signal. Our analyses suggest a complex and spatially heterogeneous relation between RSNC and CBF across different functional networks and provide preliminary evidence that spatial distribution of neuroreceptors and cerebrovascular architecture play a role in dissociative relations between regional cerebral perfusion and functional connectivity across the brain.

One aim of this study was to investigate associations between CBF and RSNC measured at baselines (i.e., pre-

drug). Overall, we did not find a ubiquitous association between these two variables (averaged over different NOIs); however, an interesting trend for association between RCNC and CBF in three NOIs—which are important for maintaining homeostasis and consciousness, namely NOI3 (auditory/somatosensory network), NOI4 (sensorimotor network) and NOI5 (default mode network)—was revealed by GEE testing of Model 1. Structures that form NOI3, such as insula, operculum, dorsocaudal ACC, somatosensory cortex, and bilateral thalamus, are implicated in physiological control and bodily awareness [Craig 2003; Critchley 2005]; the sensorimotor brain structures (NOI4) have complex hierarchical connections through basal ganglia and cerebellum to peripheral nervous system and play an important role in physiological functions such as breathing control [Pattinson et al., 2009]; and the default mode network is also known to be metabolically more 'active' than the rest of the brain 'at rest', presumably in order to keep the body in a state of adaptive consciousness to maintain the homeostatic and cognitive stability [Raichle et al., 2001]. Therefore, a closer link (compared to other NOIs) between the baseline CBF and the baseline RSNC in these networks could indicate a tighter coupling between the hemodynamic and the metabolic mechanisms of these regions—plausibly related to their primary function in adaptive regulation of consciousness states.

Another objective of the current analysis was to test how different drugs with different target receptors and different peripheral actions changed the patterns of baseline CBF/RSNC relationships. Our cross-over pharmacological experiment allowed us to test how a nonspecific physiological response (e.g., significant change in respiration rate—that as we have shown before, accounts for as high as 17% increase in cerebral perfusion [Khalili-Mahani et al., 2011a]—versus a regional electrophysiological effect (at the site of the drug target receptors), would disrupt the baseline relations between CBF and intrinsic BOLD fluctuations. As Figure 2 illustrates, Model 2 estimated a significant associations between average CBF and RSNC within NOI6 (salience/executive control) and NOI7 (working memory) after drug administration. In our models, we did not examine the drug-by-time interactions with the slope of RSNC/CBF relations; however, a negative correlation between RSNC and CBF in some of the networks is present independent of the drug condition. This observation of spatial heterogeneity of the CBF/RSNC relationship in our analysis prompted the question whether variation in CBF and RSNC were explained by similar experimental factors. This was not the case either. Testing Model 3 for CBF and RSNC independently revealed that each variable was sensitive to different model parameters. Whereas the drug-by-time interaction effect on CBF was significant for all NOIs, the interaction effects on RSNC were limited to NOIs 4 (with main effect due to drug) and to NOI8 (where main effect was due to time). This was also the case in the post-hoc ROI conjunction analysis, where overlapping drug

effects on the statistical maps of drug effects on CBF and connectivity showed a consistent increase in CBF but a heterogeneous pattern of RSNC change across different brain areas (Fig. 4). In sum, not only drug conditions disrupted the baseline relations between RSNC and CBF, but they also interacted with each metric in a spatially heterogeneous way. These observations provide evidence that the sources of variation in these two metrics are different, corroborating earlier findings that the neurophysiological substrates of drug effects on functional connectivity are spatially heterogeneous [Volkow et al., 2008].

There are two likely explanations for the spatial heterogeneity of our observations: the spatial distribution of neuroreceptors and regional differences in cerebrovascular architecture and hemodynamics. Dissociable effects of morphine on NOI6 and NOI4 are particularly noteworthy. Functionally, NOI4 includes regions of the lateral (involved in sensory aspects) and NOI6 includes regions of the medial (involved in affective and attentional aspects) of pain processing [Peyron et al., 1999; Zubieta et al., 2001], and their significant neuronal response to morphine is expected. However, as Figure 2 illustrates, the direction of CBF and RSNC covariations in these two networks are not similar. This dissociation can also be seen in the post-hoc analysis. Whereas the amplitudes of both RSNC and CBF increase in the central gyrus (which lies within NOI4, Fig. 4A), CBF in the anterior cingulate cortex (ACC) (which lies within NOI6) increases while the RSNC of the same region decreases (Fig. 4C). One possible explanation might be that the ACC (which is part of NOI6) has a high opiodergic binding potential while the sensory motor regions (which form NOI4) have a much lower binding potential for the opioid receptors [Baumgartner et al., 2006]. Therefore the electrophysiology and hence the coupling between the regional metabolic and hemodynamic responses to an opiodergic drug might be different in regions that activate these receptors. Another explanation might be that the two networks have different underlying cerebrovascular architecture/dynamics that breaks the hemodynamic/metabolic coupling in cases of acute autoregulating vascular response to drugs. In this particular case, morphine caused a significant drop in respiration rate triggering an autoregulative response to the hypercapnic condition resulting form the respiratory depression [MacIntosh et al., 2008; Pattinson et al., 2009], and hence causing up to 17% increase in total cerebral perfusion—as we reported before [Khalili-Mahani et al., 2011a]. As can be seen in Figure 3, whereas the CBF and RSNC are notably dissociated in NOI4, they are significantly correlated in NOI6. Interestingly, the baseline (i.e., predrug) association between respiration rates and RSNC was only significant in NOI4. Even after modeling drug-by-time, the relation between respiration rate and NOI4 was marginally significant ($P < 0.009$).

Comparing alcohol and morphine effects also points in the direction of our speculation that the local actions of neuroreceptors may have played a role in modulating RSNC. In general, alcohol effects on both functional connectivity and cerebral perfusion were smaller than those of morphine. Alcohol's psychoactive effects are mainly mediated through GABAergic receptors [Hanchar et al., 2006] that are distributed across the brain. As we have shown before, compared with morphine, the between subject variability in the pharmacodynamic profile of alcohol effects is larger [see Khalili-Mahani, et al., 2011a for details], and no consistent relation between physiological factors and cerebral perfusion is present. As can be seen in the post-hoc conjunction analysis, the directions of alcohol effect on both RSNC and CBF in the visual and somatosensory networks, where correlations of BOLD with intoxicating effects of alcohol are previously reported [Calhoun et al., 2004a,b; Meda et al., 2009; Van Horn et al., 2006; Volkow et al., 2008; Wang et al., 2000]—are similar (Fig. 4D,E)—although no significant interactions with the RSNC/CBF relations can be seen (Fig. 2).

Our methodological constraints preclude conclusive biological interpretations, but these findings may have important implications in emerging calibrated-BOLD experiments under pharmacological interventions that aim to address the issue of CBF/BOLD coupling [Asghar et al., 2011; Chen and Parrish, 2009a,b; Grichisch et al., 2011; Griffeth et al., 2011; Perthen et al., 2008; Qiu et al., 2008a; Qiu et al., 2008b; St Lawrence et al., 2003]. Previously, it has been shown that relatively mild pharmacological intervention with caffeine [Chen and Parrish 2009b; Griffeth et al., 2011; Perthen et al., 2008] or indomethacin [St Lawrence et al., 2003] leads to a different CBF/BOLD coupling compared to tasks. It has also been shown that the dynamics of pharmacological alterations to CBF/BOLD coupling differ across brain regions [Luchtmann et al., 2010; Qiu et al., 2008a; Qiu et al., 2008b]. Currently, little is known about the BOLD/CBF coupling in relation to resting-state functional connectivity (except that it has been shown that similar functional network topographies may be also detected from analyzing the time course of ASL data [Chuang et al., 2008; Zou et al., 2009]. As increasing evidence emerges in support of the notion that the receptor finger-prints across the brain play a role in defining its functional configuration [Zilles and Amunts, 2010], prototypical studies such as ours might provide preliminary data about the relation between regional CBF and functional connectivity, to help refine further quantitative studies of how drugs modulate the neuronal and hemodynamic coupling.

As far as the question of the better biomarker for early phases of drug research is concerned, our results indicate that RSfMRI and PCASL are sensitive to different aspects of drug effects on the brain. Whereas CBF seems sensitive to drug-by-time interaction effects in almost all brain areas (perhaps relating to general vascular response to drugs), RSNC is more sensitive to time effects and reveals more focal effects compared to CBF (perhaps relating to specific functional states). In our study, PCASL data provided more statistical power than RSfMRI in detecting drug-by-

time interactions. However, RSfMRI results were anatomically more distinct, partly because of temporal and spatial resolution of RSfMRI. Note that RSfMRI and PCASL data are not acquired at the same aperture resolution (3.44 mm isotropic resolution for RSfMRI versus $3 \times 3 \times 7$ mm$_3$ resolution for PCASL that leads to increased partial volume effects)—although we showed that including the partial gray matter volume as a weighting factor in GEE modeling did not change the outcome of our observations. Further studies are needed to examine how such effects influence the spatial distribution of effect clusters and the sensitivity of each measure.

One possible explanation for the higher statistical sensitivity of CBF versus RSNC is that the baseline global CBF seems to be stable between different measurements of the same subject [Khalili Mahani et al., 2011a]. Thus a smaller within-subject and between-condition variation in the baseline measures would increase the sensitivity of the model to minute CBF changes after drug administration. On the other hand, RSNC depends on patterns of BOLD fluctuations over time, which likely follows the patterns of neuronal activity [Mantini et al., 2007] and might be less stable than CBF across repeated baseline measurements of the same subject. In addition, whereas CBF values reflect the average amount of arterial blood flowing into a given voxel over 1 min, RSNC values reflect a statistical estimation of how low frequency BOLD fluctuations in one region, are similar to those in another region or a given NOI. In other words, CBF may be more suitable to detect the primary site of drug action, whereas RSNC would be more suitable to detect adaptive changes in effective connectivity of the brain networks. Since model-optimization, that aims to capture the slightest pharmacologically induced variations in the brain, is a critical aspect of drug research [Pendse et al., 2010] RSNC and CBF might provide complementary information for pharmacokinetic/pharmacodynamic (PK/PD) modeling.

An important limitation of this study is that it is intended as a proof-of-principle; thus some standardization features such as dimension-reduction and network-based analytical approach prohibit general conclusions. However, despite reducing the spatiotemporal NOI signals to one variable per network, and testing them as independent variables with relatively simple GEE models, we could detect effects that were also present in the more rigorous voxel-based statistical testing of drug effects. Therefore, NOI-averaged RSNC and CBF values may be useful pharmacodymanic endpoints in computationally intensive PK/PD modeling. However, interpretative limitations of RSNC as an index of network consistency must be noted. RSNC does not characterize the amplitude of low-frequency fluctuations (ALFF) or the local synchrony and regional homogeneity (ReHo) of BOLD or dynamic CBF fluctuations, which seem to correlate with static CBF (in the default mode network) [Li et al., 2012; Zou et al., 2009]. The advantage of RSNC compared to other resting-state measures is that the dual regression method partials out the common variations across network and as such provides an index of NOIs dynamics independent of global transient factors such as global CBF increase or physiological noise.

In conclusion, our results emphasize the importance of considering the spatial heterogeneity of CBF/connectivity variations. Such considerations benefit model-optimization and hypothesis testing in early phases of pharmacological studies. They are also important in quantitative studies of cerebrovascular and metabolic coupling of brain function under pharmacological stimulation. The observation of the spatial heterogeneity and model-dependency of RSNC and CBF correlations under different CNS drugs such as morphine and alcohol versus placebo encourages further inquiries into the neurological factors such as vascular architecture, flow territories or receptor fingerprints that distinguish these commonly detected network topographies. Under current limitations, RSfMRI and PCASL provide complementary information about the dynamics of brain's hemodynamic responses to drugs. Given the differential sensitivity of these methods, acquiring RSfMRI and ASL data together in pharmacological studies is recommended.

REFERENCES

Asghar MS, Hansen AE, Pedersen S, Larsson HB, Ashina M (2011): Pharmacological modulation of the bOLD response: A study of acetazolamide and glyceryl trinitrate in humans. J Magn Resonance Imaging JMRI 34: 921–927.

Baumgartner U, Buchholz HG, Bellosevich A, Magerl W, Siessmeier T, Rolke R, Hohnemann S, Piel M, Rosch F, Wester HJ,et al.(2006): High opiate receptor binding potential in the human lateral pain system. NeuroImage 30: 692–699.

Becerra L, Harter K, Gonzalez RG, Borsook D (2006): Functional magnetic resonance imaging measures of the effects of morphine on central nervous system circuitry in opioid-naive healthy volunteers. Anesthesia Analgesia 103:208-216, table of contents.

Becerra L, Schwartzman RJ, Kiefer RT, Rohr P, Moulton EA, Wallin D, Pendse G, Morris S, Borsook D (2009): CNS measures of pain responses pre- and post-anesthetic ketamine in a patient with complex regional pain syndrome. Pain Med. Epub ahead of print; DOI: 10.1111/j.1526-4637.2009.00559.

Beckmann CF, DeLuca M, Devlin JT, Smith SM (2005): Investigations into resting-state connectivity using independent component analysis. Philos Trans Roy Soc Lond Series B, Biol Sci 360: 1001–1013.

Biswal BB, Mennes M, Zuo XN, Gohel S, Kelly C, Smith SM, Beckmann CF, Adelstein JS, Buckner RL, Colcombe S,et al.(2010): Toward discovery science of human brain function. Proc Natl Acad Sci USA 107: 4734–4739.

Blaha M, Aaslid R, Douville CM, Correra R, Newell DW (2003): Cerebral blood flow and dynamic cerebral autoregulation during ethanol intoxication and hypercapnia. J Clin Neurosci 10: 195–198.

Borsook D, Hargreaves R, Becerra L (2011):Can functional magnetic resonance imaging improve success rates in CNS drug discovery? Expert Opin Drug Discov 6: 597–617.

Brookes MJ, Woolrich M, Luckhoo H, Price D, Hale JR, Stephenson MC, Barnes GR, Smith SM, Morris PG (2011): Investigating the electrophysiological basis of resting state networks using magnetoencephalography. Proc Natl Acad Sci USA 108: 16783–16788.

Buxton RB, Frank LR, Wong EC, Siewert B, Warach S, Edelman RR (1998): A general kinetic model for quantitative perfusion imaging with arterial spin labeling. Magn Resonance Med 40: 383–396.

Calhoun VD, Altschul D, McGinty V, Shih R, Scott D, Sears E, Pearlson GD (2004a): Alcohol intoxication effects on visual perception: An fMRI study. Hum Brain Mapp 21: 15–26.

Calhoun VD, Pekar JJ, Pearlson GD (2004b): Alcohol intoxication effects on simulated driving: Exploring alcohol-dose effects on brain activation using functional MRI. Neuropsychopharmacology 29: 2097–2017.

Chen Y, Parrish TB (2009a): Caffeine dose effect on activation-induced BOLD and CBF responses. Neuroimage 46: 577–583.

Chen Y, Parrish TB (2009b): Caffeine's effects on cerebrovascular reactivity and coupling between cerebral blood flow and oxygen metabolism. Neuroimage 44: 647–652.

Chuang KH, van Gelderen P, Merkle H, Bodurka J, Ikonomidou VN, Koretsky AP, Duyn JH, Talagala SL (2008): Mapping resting-state functional connectivity using perfusion MRI. Neuroimage 40: 1595–1605.

Cole DM, Smith SM, Beckmann CF (2010): Advances and pitfalls in the analysis and interpretation of resting-state FMRI data. Frontiers Syst Neurosci 4: 8.

Craig AD (2003): Interoception: the sense of the physiological condition of the body. Curr Opin Neurobiol 13: 500–505.

Critchley HD (2005): Neural mechanisms of autonomic, affective, and cognitive integration. J Comp Neurol 493: 154–166.

Dai W, Garcia D, de Bazelaire C, Alsop DC (2008): Continuous flow-driven inversion for arterial spin labeling using pulsed radio frequency and gradient fields. Magn Resonance Med 60: 1488–1497.

Damoiseaux JS, Rombouts SA, Barkhof F, Scheltens P, Stam CJ, Smith SM, Beckmann CF (2006): Consistent resting-state networks across healthy subjects. Proc Natl Acad Sci USA 103: 13848–13853.

Davis TL, Kwong KK, Weisskoff RM, Rosen BR (1998): Calibrated functional MRI: Mapping the dynamics of oxidative metabolism. Proc Natl Acad Sci USA 95: 1834–1839.

Grichisch Y, Cavusoglu M, Preissl H, Uludag K, Hallschmid M, Birbaumer N, Haring HU, Fritsche A, Veit R (2011): Differential effects of intranasal insulin and caffeine on cerebral blood flow. Hum Brain Mapp 33:280–287.

Griffeth VE, Perthen JE, Buxton RB (2011): Prospects for quantitative fMRI: investigating the effects of caffeine on baseline oxygen metabolism and the response to a visual stimulus in humans. NeuroImage 57: 809–816.

Hanchar HJ, Chutsrinopkun P, Meera P, Supavilai P, Sieghart W, Wallner M, Olsen RW (2006): Ethanol potently and competitively inhibits binding of the alcohol antagonist Ro15-4513 to alpha4/6beta3delta GABAA receptors. Proc Natl Acad Sci USA 103: 8546–8551.

Hoge RD, Atkinson J, Gill B, Crelier GR, Marrett S, Pike GB (1999): Investigation of BOLD signal dependence on cerebral blood flow and oxygen consumption: The deoxyhemoglobin dilution model. Magn Resonance Med 42: 849–863.

Khalili-Mahani N, van Osch MJ, Baerends E, Soeter RP, de Kam M, Zoethout RW, Dahan A, van Buchem MA, van Gerven JM, Rombouts SA (2011a): Pseudocontinuous arterial spin labeling reveals dissociable effects of morphine and alcohol on regional cerebral blood flow. J Cerebral Blood Flow Metabolism 31: 1321–1333.

Khalili-Mahani N, Zoethout RM, Beckmann CF, Baerends E, de Kam ML, Soeter RP, Dahan A, van Buchem MA, van Gerven JM, Rombouts SA (2011b): Effects of morphine and alcohol on functional brain connectivity during "resting state": A placebo-controlled crossover study in healthy young men. Hum Brain Mapp 33:1003–1018.

Khalili-Mahani N, Chang C, van Osch MJ, Veer IM, van Buchem MA, Dahan A, Beckmann CF, van Gerven JM, Rombouts SA (2012): The impact of "physiological correction" on functional connectivity analysis of pharmacological resting state fMRI. NeuroImage 65C:499–510.

Kim SG, Rostrup E, Larsson HB, Ogawa S, Paulson OB (1999): Determination of relative CMRO2 from CBF and BOLD changes: Significant increase of oxygen consumption rate during visual stimulation. Magn Resonance Med 41: 1152–1161.

Li Z, Zhu Y, Childress AR, Detre JA, Wang Z (2012): Relations between BOLD fMRI-derived resting brain activity and cerebral blood flow. PloS One 7: e44556.

Liang KY, Zeger SL (1986): Longitudinal data-analysis using generalized linear-models. Biometrika 73: 13–22.

Luchtmann M, Jachau K, Tempelmann C, Bernarding J (2010): Alcohol induced region-dependent alterations of hemodynamic response: Implications for the statistical interpretation of pharmacological fMRI studies. Exp Brain Res 204: 1–10.

MacIntosh BJ, Pattinson KT, Gallichan D, Ahmad I, Miller KL, Feinberg DA, Wise RG, Jezzard P (2008): Measuring the effects of remifentanil on cerebral blood flow and arterial arrival time using 3D GRASE MRI with pulsed arterial spin labelling. J Cerebral Blood Flow Metabolism 28: 1514–1522.

Mantini D, Perrucci MG, Del Gratta C, Romani GL, Corbetta M (2007): Electrophysiological signatures of resting state networks in the human brain. Proc Natl Acad Sci USA 104: 13170–13175.

Margulies DS, Vincent JL, Kelly C, Lohmann G, Uddin LQ, Biswal BB, Villringer A, Castellanos FX, Milham MP, Petrides M (2009): Precuneus shares intrinsic functional architecture in humans and monkeys. Proc Natl Acad Sci USA 106: 20069–20074.

Meda SA, Calhoun VD, Astur RS, Turner BM, Ruopp K, Pearlson GD (2009): Alcohol dose effects on brain circuits during simulated driving: an fMRI study. Hum Brain Mapp 30: 1257–1270.

Nichols T, Brett M, Andersson J, Wager T, Poline JB (2005): Valid conjunction inference with the minimum statistic. NeuroImage 25: 653–660.

O'Connor S, Morzorati S, Christian J, Li TK (1998): Clamping breath alcohol concentration reduces experimental variance: Application to the study of acute tolerance to alcohol and alcohol elimination rate. Alcoholism Clin Exp Res 22: 202–210.

Ogoh S, Tzeng YC, Lucas SJ, Galvin SD, Ainslie PN (2010):Influence of baroreflex-mediated tachycardia on the regulation of

dynamic cerebral perfusion during acute hypotension in humans.. J Physiol 588(Part 2): 365–371.

Pan W (2001): Model selection in estimating equations. Biometrics 57: 529–534.

Pattinson KT, Governo RJ, MacIntosh BJ, Russell EC, Corfield DR, Tracey I, Wise RG (2009): Opioids depress cortical centers responsible for the volitional control of respiration. J Neurosci 29: 8177–8186.

Pattinson KT, Rogers R, Mayhew SD, Tracey I, Wise RG (2007): Pharmacological FMRI: Measuring opioid effects on the BOLD response to hypercapnia. J Cerebral Blood Flow Metabolism 27: 414–423.

Pendse GV, Schwarz AJ, Baumgartner R, Coimbra A, Upadhyay J, Borsook D, Becerra L (2010): Robust, unbiased general linear model estimation of phMRI signal amplitude in the presence of variation in the temporal response profile. J Magn Resonance Imaging 31: 1445–1457.

Perthen JE, Lansing AE, Liau J, Liu TT, Buxton RB (2008): Caffeine-induced uncoupling of cerebral blood flow and oxygen metabolism: A calibrated BOLD fMRI study. NeuroImage 40: 237–247.

Peyron R, Garcia-Larrea L, Gregoire MC, Costes N, Convers P, Lavenne F, Mauguiere F, Michel D, Laurent B (1999): Haemodynamic brain responses to acute pain in humans: Sensory and attentional networks. Brain 122 (Part 9):1765–1780.

Qiu M, Ramani R, Swetye M, Constable RT (2008a): Spatial non-uniformity of the resting CBF and BOLD responses to sevoflurane: In vivo study of normal human subjects with magnetic resonance imaging. Hum Brain Mapp 29: 1390–1399.

Qiu M, Ramani R, Swetye M, Rajeevan N, Constable RT (2008b): Anesthetic effects on regional CBF, BOLD, and the coupling between task-induced changes in CBF and BOLD: An fMRI study in normal human subjects. Magn Resonance Med 60: 987–996.

Rack-Gomer AL, Liau J, Liu TT (2009): Caffeine reduces resting-state BOLD functional connectivity in the motor cortex. NeuroImage 46: 56–63.

Raichle ME, MacLeod AM, Snyder AZ, Powers WJ, Gusnard DA, Shulman GL (2001): A default mode of brain function. Proc Natl Acad Sci USA 98: 676–682.

Sarton E, Olofsen E, Romberg R, den Hartigh J, Kest B, Nieuwenhuijs D, Burm A, Teppema L, Dahan A (2000): Sex differences in morphine analgesia: An experimental study in healthy volunteers. Anesthesiology 93:1245–1254; discussion 6A.

Smith SM, Fox PT, Miller KL, Glahn DC, Fox PM, Mackay CE, Filippini N, Watkins KE, Toro R, Laird AR,et al.(2009): Correspondence of the brain's functional architecture during activation and rest. Proc Natl Acad Sci USA 106: 13040–13045.

Smith SM, Miller KL, Salimi-Khorshidi G, Webster M, Beckmann CF, Nichols TE, Ramsey JD, Woolrich MW (2011): Network modelling methods for FMRI. NeuroImage 54: 875–891.

St Lawrence KS, Ye FQ, Lewis BK, Frank JA, McLaughlin AC (2003): Measuring the effects of indomethacin on changes in cerebral oxidative metabolism and cerebral blood flow during sensorimotor activation. Magn Resonance Med 50: 99–106.

Van Horn JD, Yanos M, Schmitt PJ, Grafton ST (2006): Alcohol-induced suppression of BOLD activity during goal-directed visuomotor performance. NeuroImage 31: 1209–1221.

van Osch MJ, Teeuwisse WM, van Walderveen MA, Hendrikse J, Kies DA, van Buchem MA (2009):Can arterial spin labeling detect white matter perfusion signal? Magn Resonance Med 6 2: 165–173.

Vincent JL, Kahn I, Van Essen DC, Buckner RL (2010): Functional connectivity of the macaque posterior parahippocampal cortex. J Neurophysiol 103: 793–800.

Volkow ND, Ma Y, Zhu W, Fowler JS, Li J, Rao M, Mueller K, Pradhan K, Wong C, Wang GJ (2008): Moderate doses of alcohol disrupt the functional organization of the human brain. Psychiatry Res 162: 205–213.

Wang DJ, Chen Y, Fernandez-Seara MA, Detre JA (2011): Potentials and challenges for arterial spin labeling in pharmacological magnetic resonance imaging. J Pharmacology Exp Therapeutics 337: 359–366.

Wang GJ, Volkow ND, Franceschi D, Fowler JS, Thanos PK, Scherbaum N, Pappas N, Wong CT, Hitzemann RJ, Felder CA (2000): Regional brain metabolism during alcohol intoxication. Alcoholism Clin Exp Res 24: 822–829.

Wise RG, Rogers R, Painter D, Bantick S, Ploghaus A, Williams P, Rapeport G, Tracey I (2002): Combining fMRI with a pharmacokinetic model to determine which brain areas activated by painful stimulation are specifically modulated by remifentanil. NeuroImage 16: 999–1014.

Wise RG, Tracey I (2006): The role of fMRI in drug discovery. J Magn Resonance Imaging 23: 862–876.

Zeger SL, Liang KY, Albert PS.1988. Models for longitudinal data—A generalized estimating equation approach. Biometrics 44: 1049–1060.

Zilles K, Amunts K (2009): Receptor mapping: Architecture of the human cerebral cortex. Current Opin Neurol 22: 331–339.

Zilles K, Amunts K (2010): Centenary of Brodmann's map—Conception and fate. Nature reviews. Neuroscience 11: 139–145.

Zilles K, Palomero-Gallagher N, Schleicher A (2004): Transmitter receptors and functional anatomy of the cerebral cortex. J Anatomy 205: 417–432.

Zoethout RW, van Gerven JM, Dumont GJ, Paltansing S, van Burgel ND, van der Linden M, Dahan A, Cohen AF, Schoemaker RC (2008): A comparative study of two methods for attaining constant alcohol levels. Br J Clin Pharmacol 66: 674–681.

Zou Q, Wu CW, Stein EA, Zang Y, Yang Y (2009): Static and dynamic characteristics of cerebral blood flow during the resting state. NeuroImage 48: 515–524.

Zubieta JK, Smith YR, Bueller JA, Xu Y, Kilbourn MR, Jewett DM, Meyer CR, Koeppe RA, Stohler CS (2001): Regional mu opioid receptor regulation of sensory and affective dimensions of pain. Science 293: 311–315.

Zuo XN, Kelly C, Adelstein JS, Klein DF, Castellanos FX, Milham MP (2010): Reliable intrinsic connectivity networks: Test-retest evaluation using ICA and dual regression approach. NeuroImage 49: 2163–2177.